RSC Advances

PAPER

View Article Online
View Journal | View Issue

Cite this: *RSC Adv.*, 2018, **8**, 36123

Removal of Au^{3+} and Ag^{+} from aqueous media with magnetic nanoparticles functionalized with squaramide derivatives†

Paulino Duel,[a] M. Susana Gutiérrez,[a] Paulina Rodríguez,[b] Alberto León,[a] Kenia A. López,[a] Jeroni Morey *[a] and M. Nieves Piña*[a]

Received 19th September 2018
Accepted 17th October 2018

DOI: 10.1039/c8ra07793b

rsc.li/rsc-advances

New magnetic hybrid nanoparticles of Fe_3O_4 coated with organosulfur-squaramide compounds are prepared. The modified-nanoparticles show a good coordination for Ag^{+} and Hg^{2+} cations in water, and present a high affinity for Au^{3+} ions. The behaviour of the squaramide-coated nanoparticles differs significantly from that previously reported for nanoparticles used as Au^{3+} scavengers. In the presence of organosulfur-squaramide, the Au^{3+} salt is reduced to gold nanoparticles that are deposited upon Fe_3O_4 nanoparticles. For the first time, the coordination capacity of the carbonyl squaramide groups with the gold cation, based on purely electrostatic cation–dipole interactions, is proved.

Introduction

In today's society, in order to maintain good harmony between progress and the environment and ensure the sustainability of our resources, industry has to use secure collection and reuse technologies – what is known as a "circular economy".[1] One of the main objectives in the field of water pollution and the environment is the recovery of metal ions, and in particular the most toxic or economically most valuable, by coordination, to prevent their spillage from becoming out of control.

The salts derived from Ag^{+} and Au^{3+} (heavy late metals) although they have a lower impact on health and the environment, than the known toxic heavy and transition metals, such as: Pb^{+2}, Hg^{+2}, Cr^{3+}, Cd^{2+}, Zn^{2+}, Co^{2+} or Cu^{2} primarily due to their minor diffusion, have recently received the attention of researchers, because there are not many technologic alternatives for their encapsulation and recovery, especially in the case of Au^{3+} salts.[2–5]

In fact, in aqueous samples derived from the anthropogenic action the concentration of the Ag^{+} and Au^{3+} salts is highly significant. A clear example is the electronic industry that, for the manufacture of its components, uses salts derived from Ni^{2+}, Pd^{2+}, Al^{3+}, Ag^{+} and Au^{3+}, even more profusely, due to the great worldwide demand of electronic devices. The salts of these metal ions, once their useful life is over, can end up in a landfill, and without the adequate control, can contaminate the aquifers of their environment. These emerging contaminants, known as e-wastes, need effective technological solutions for their encapsulation and collection, either for public health or economic reasons. Therefore it is necessary to develop new materials that could offer a bigger capacity, and especially a better selectivity in their encapsulation and elimination from the environment.

Typically, the leaching method (oxidation/cyanidation with cyanide salts) has been used for the recovery of gold and silver. This is an extremely toxic and polluting process,[6] which transforms Au^{0} or Ag^{0} into the $Au(CN)_2^{-}$ and $Ag(CN)_2^{-}$ water soluble coordination complexes. Recently, it has been proposed a more green-friendly method, based on the precipitation of the salts of Au^{3+} in water, as $KAuBr_4$, with α-cyclodextrins.[7,8] Another smart proposal for recovery of Au^{+} and Au^{3+} consists in the formation of a Metal Organic Framework (MOF) functionalized with L-methionine.[9]

The magnetic iron oxide nanoparticles of Fe_3O_4 (FeNP) are inorganic material, easily modifiable and easily to functionalize using simple synthetic processes. The union between the organic receptor and the FeNP is established using well known linker molecules, which contain the silane group such as APTES (3-aminopropyltriethoxysilane) that forms bonds of the Si–O–Fe type,[10,11] or, with structures derived from catechol, such as L-DOPA[12] or dopamine,[13,14] which form stable bonds of the Ar–O–Fe type. This functionalization prevents the aggregation of the FeNP, procures a good dispersion in a neutral aqueous medium and protects against the leaching of the FeNP.

The FeNP are an economically accessible and biocompatible material that can be obtained with well defined morphological properties, conveniently adjusting the experimental conditions during the preparation,[15] with a high surface area per mass,

[a]*Department of Chemistry, University of the Balearic Islands, Crta. de Valldemossa Km. 7.5, 07122, Spain. E-mail: jeroni.morey@uib.es; neus.pinya@uib.es*

[b]*Laboratorio de Análisis Clínicos, Dirección de Servicios Tecnológicos, Centro de Innovación Aplicada en Tecnologías Competitivas (CIATEC, A. C.), Omega 201, Industrial Delta, 37545 León, Guanajuato, México*

† Electronic supplementary information (ESI) available: SEM microphotographs, DLS, *Z*-potential, FTIR, TGA, ^{1}H RMN, ^{13}C RMN, HRMS-ESI. See DOI: 10.1039/c8ra07793b

around 100 $m^2\ g^{-1}$. In addition, the FeNP are an active support, since it has been shown that certain contaminants adsorb onto its surface.[16,17] If this feature is combined with their inherent magnetic properties, the functionalized FeNP represent a hybrid nanomaterial that offers certain advantages in the separation process, compared with other supports used for this purpose.[16] In this case, the recovery of contaminating metal ions present in aqueous samples can be carried out easily, by magneto filtration of the hybrid material, separating the metal ions from the aqueous sample. This procedure is based on two complementary processes: first, on the coordination capacity between the metal ion and the organic receptor; and second, on the contribution of the adsorption of contaminants on the bare surface of FeNP.

Recently, we have demonstrated the efficacy of dopamine-squaramide iron oxide nanoparticles as adsorbent for different toxic heavy metal contaminants in aqueous systems.[18] In addition, we have reported a recyclable nanomaterial based on bisimide perylene dopamine for the removal of 15 carcinogenic polycyclic aromatic compounds (PAHs) from aqueous media by magneto filtration.[19]

Results and discussion

Taking into account our previous research, the aim of this work is to improve the model in order to increase the degree of interaction of the functionalized nanoparticles with the metal ions of interest. Thus, in the present study we report the comparison of four squaramide-coated nanoparticles FeNP-SQ(1–4), see Fig. 1, that present the ability to coordinate some metallic ions, through the carbonyl groups of the squaramide ring. This strong coordination becomes evident, for example, with metal ions such as Hg^{2+} or Pb^{2+}.[18] Moreover, to further enhance the coordination ability of FeNP-SQ towards the Hg^{2+} and Pb^{2+} ions, three new materials derived from squaramide have been prepared, also, to widen the study to new ions such as Ag^{+} and Au^{3+}. Taking advantage of the great affinity that these metal cations have for the sulfur group derivatives,[20,21] a thiomethyl ether and disulfide groups have been incorporated in two (FeNP-SQ2 and FeNP-SQ3) and one (FeNP-SQ4) of these new nanoparticles, respectively. Furthermore, the FeNP-SQ1 receptor, which has already previously described,[18] is used in this study for comparative purposes, to evaluate the usefulness of the introduction of chains functionalized with sulfur derivatives in the di-squaramide. In addition, never previously described tests have been carried out with the hybrid material FeNP-SQ1 with metal salts of Ag^{+} and Au^{3+}.

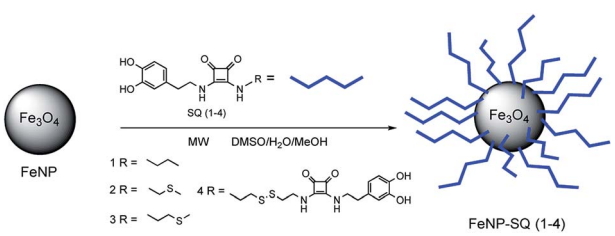

Fig. 1 Structure of the four, FeNP-SQ(1–4), hybrid derivatives used in this work.

The presence of the iron nanoparticle core in the new materials, together with the fact that they are not soluble, makes impossible to carry out recognition studies using certain techniques, such as ^{1}H NMR spectroscopy, *e.g.* by observation of the complexation induced shifts (CIS). For this reason, besides the proposed models, the synthesis of the corresponding derivatives of 3,4-dimethoxy dopamine (SQ5, SQ6, SQ7, Fig. 2 and 3) was carried out. These new materials are easy to handle in solution, a fact that will allow us to observe the changes in chemical shift ($\Delta\delta$) of certain signals, indicating a possible supramolecular interaction. It is expected that the interaction of the "free" model (SQ5, SQ6 and SQ7) with the ions will be much weaker than with the "supported" models, since the number of interaction sites is greater in the functionalized nanoparticle.

The organic receptors SQ2 and SQ3, di-squaramide-thioether derivatives containing one dopamine, and the SQ5 and SQ6 receptors also with a di-squaramide-thioether group containing one 3,4-dimethoxy dopamine, were prepared from diethyl squarate by two alternative routes, as shown in Fig. 2.

The mono-squaramides are synthesized, with good yields, by adding a primary amine to the diethyl squarate, controlling the temperature, the type of solvent (diethyl ether or acetonitrile), and the number of equivalents of amine added. With these experimental conditions we avoid obtaining the double entry product.[22,23] In this study, in addition to 3,4-dimethoxy dopamine, 2-(methylthio)ethan-1-amine, or 3-(methylthio) propan-1-amine have been used as sulfur derivatives to coordinate the FeNP. Finally, the di-squaramide – introduction of the second amine in the ring of the mono-squaramide – is obtained from the mono-squaramide using a more polar solvent, such as MeOH or EtOH, in the presence of an equivalent of another primary amine. In this way, disquaramides with different substitution are obtained on each side of the squaric ring.

On the other hand, the synthetic route for obtaining the bis-disquaramides SQ4, with two units of dopamine, or the 3,4-dimethoxy dopamine SQ7, each linked by a chain with a disulfide group, starts with a common intermediate, obtained by the

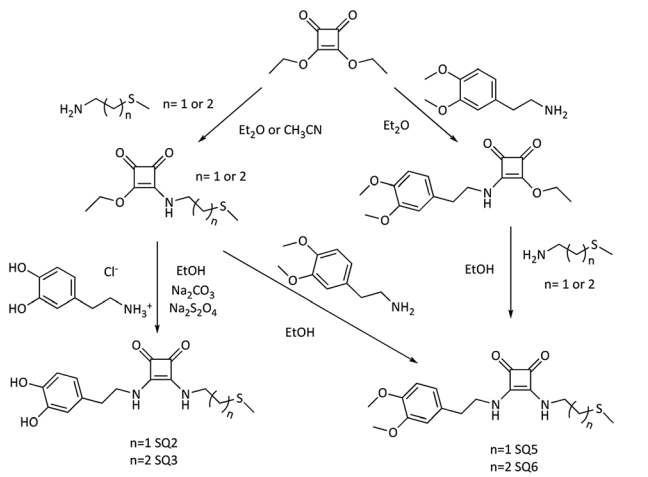

Fig. 2 Synthesis of di-squaramide-dopamine-thioether and di-squaramide-thioether-3,4-dopamine receptors.

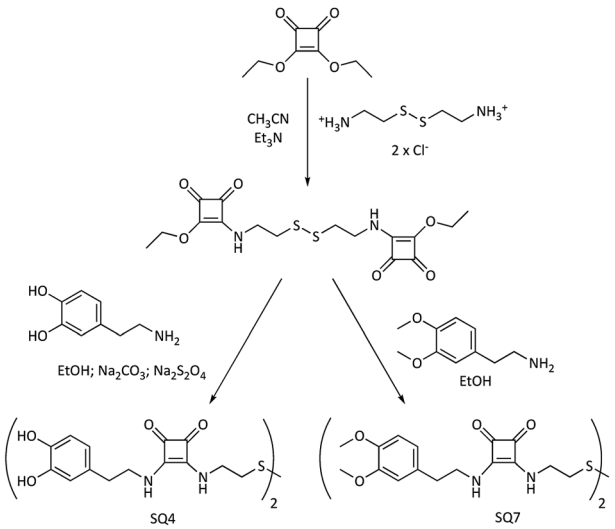

Fig. 3 Synthesis of bis-di-squaramide-dopamine-disulfide and bis-di-squaramide-3,4-dopamine-disulfide receptors.

condensation of diethyl squarate with cystamine, as shown in Fig. 3.

In a standard process, the synthesis of the squaramide-hybrid nanomaterials, FeNP-SQ(2–4) initiates with the scatter of FeNP nanoparticles in methanol (6 mL) inside a 2–5 mL microwave vessel. At that point, the squaramide-dopamine derivatives SQ2, SQ3 or SQ4, previously dissolved in 1 mL of DMSO, are added. The reaction tube is hermetically closed and inserted in the microwave.[24–26] The reaction is carried out during 20 minutes, at 120 °C, obtaining in these conditions a pressure about 3 bars. After reaction, functionalized magnetic nanoparticles are cleaned with water (3 × 10 mL) and suspended in 10 mL of methanol, in a dark vial and stored in a freezer, to ensure its conservation.

In this research, we used magnetic nanoparticles of Fe_3O_4 prepared by co-precipitation. Despite having a larger size and dispersivity than those prepared by other methods,[15] these Fe_3O_4 nanoparticles are a very attractive alternative, because from a preparatory point of view, they are simpler, cheaper and faster to synthesize. They present an excellent dispersivity in aqueous medium and a great functionalization capacity with the new SQ receptors (1–4).

The shape and size distribution of the new hybrid nanomaterials were analysed using the Scanning Electron Microscope (SEM), Dynamic Light Scattering (DLS) and zeta potential (see Fig. SI-1A–C†). The results are shown in Table 1. All of them present a very uniform iron oxide core about 41 nm, of spherical shape nanoparticles. The measurements obtained by DLS, point out average hydrodynamic diameters between 220 and 325 nm, with a low degree of polydispersity index (PdI). The *Z*-potential has a significant negative charge, at pH = 6.5, which is in agreement with its good dispersity observed in water.

To verify that the modification of the surface of the magnetite nanoparticle was adequate, the spectra by Fourier-Transform Infrared Spectroscopy (FTIR) were recorded. The structure of these new hybrids nanomaterial, FeNP-SQ(1–4), is characterized by showing two C=O stretching bands, located at

Table 1 Average sizes calculated by SEM and DLS of each of the new nanoparticles

	SEM (nm)	DLS	PdI	*Z*-Potential
FeNP	40.0	285.4	0.248	−24 mV
FeNP-SQ1	45.2	229.0	0.378	−46 mV
FeNP-SQ2	40.7	224.5	0.169	−41 mV
FeNP-SQ3	41.9	255.0	0.258	−28 mV
FeNP-SQ4	38.0	321.9	0.266	−22 mV

1799–1800 cm^{-1} and 1652 cm^{-1} characteristic of the squaramide moiety. At 1590–1591 cm^{-1} there is an intense band assigned to N–H bending of the amide of squaramide. The characteristic bands of the bond between Fe and O appear at 576–602 cm^{-1} and 438–453 cm^{-1}. The thiomethyl S–Me band is located at 1353 cm^{-1}. The comparison between the spectra of the different materials is shown in the ESI (see Fig. SI-2†).

The Thermogravimetric Analysis (TGA) shows a single weight loss, between 200 and 900 °C. The functionalization percentages calculated for each of the materials are shown in Table 2[25] (see Fig. SI-3†).

In general, the percentage of functionalization is calculated between 40 and 50%, according to previous works already published,[26] and with a good number of receptors per unit of area. However, judging from the obtained results, two features are worth mentioning: on the one hand, the high functionalization of the FeNP-SQ1 compared to the original recipe already published, 4 receptors per nm^2 *versus* 93 receptors per nm^2 calculated in this work. This increase is due to the improvement of the original methodology, by using microwave techniques that considerably increases the functionalization percentage.[26] On the other hand, the relatively low functionalization of the FeNP-SQ4. The bis-di-squaramide SQ4 contains two dopamine units initially arranged to form a union between two nanoparticles, and thus form a network capable of interacting more effectively with the metal ions. The fact that in the SEM it is observed that the size of the FeNP-SQ4 nanoparticles is comparable to the rest and that the functionalization of the FeNP-SQ4 is half that of FeNP-SQ2 and FeNP-SQ3, leads us to propose that, actually, the two anchor points are on the same nanoparticle, forming a cycle on the surface of the solid.

This coordination proposal is in agreement with previous works of our research group that support that, in solution, flexible di-squaramides are folded on themselves, due to interaction between the two units of squaramides, thus favouring

Table 2 Thermogravimetric results: calculation of functionalization of iron oxide nanoparticles

	T, °C	Weight loss (%)	Number molecules/nm^2
FeNP-SQ1	200–850	49	94
FeNP-SQ2	200–800	42	48
FeNP-SQ3	200–890	43	44
FeNP-SQ4	200–800	40	23

anchoring on the nanoparticle surface and preventing its anchoring on two surfaces of different nanoparticles.[27]

To verify the involvement of the SMe or disulfide S–S groups of the FeNP-SQ(2–4) in the molecular recognition process with the metal ions of interest, the di-squaramide derived from the 3,4-dimethoxy dopamine were used SQ(5–7), for a comparative study by using ^{1}H-NMR. These three compounds have the same side chains as the hybrid material FeNP-SQ(2–4) and are soluble in organic media, which will allow us to use them as suitable models for this part of the study. The nuclear magnetic resonance experiments were carried out in DMSO-d_6 comparing the displacement of the proton signals, when separately adding, the following metal salts: $Hg(ClO_4)_2$, $Pb(ClO_4)_2$, $AgNO_3$, $AuCl_3\cdot 3H_2O$ to the SQ receptors (5–7), in a stoichiometric ratio 1 : 1 (receptor/metal ion). These ^{1}H-NMR spectra were recorded every 15 minutes, during the first hour; then after 2, 4, and 6 hours; and finally after 24 and 48 hours.

From these ^{1}H-NMR experiments interesting conclusions are drawn about the mode of interaction of the metal ion with the di-squaramide. In Fig. SI-4A and SI-4B,† the ^{1}H-NMR spectra recorded by adding $Hg(ClO_4)_2$ to the SQ5 and SQ6 receptor are compared, respectively. A downfield induced chemical shift changes are clearly observed for the protons directly bonded to the carbon with the sulfur atom, $\Delta\delta = 0.1$ ppm (SQ5 receptor) and $\Delta\delta = 0.4$ ppm (SQ6 receptor), for the methyl singlet of Me-S. Other changes include a $\Delta\delta = 0.1$ ppm (SQ5 receptor) and $\Delta\delta =$ 0.3 ppm (SQ6 receptor) for the ethyl CH_2 triplet. The remaining signals of the SQ6 receptor (the protons in the carbons marked 8 and 9), also show a low downfield shift. The rest of the proton signals of the molecule are not affected, *e.g.* OCH_3 aromatic groups. This leads us to propose that the sulfur atom, in this receptor, is an active part of the molecular recognition of Hg^{2+}. In previous studies, the formation of an organomercury compound was documented, resulting from an aromatic electrophilic substitution on the 3,4-dimethoxy dopamine ring of SQ1 receptor.[18] However, in the present study, the aromatic zone of the receptors does not undergo any changes in the ^{1}H-NMR spectra, thus discarding the formation of organomercury species. These results can be related to the solvent chosen to carry out the experiments, DMSO in the present work and acetonitrile in previous studies, where the latter solvent seems to favour especially this type of aromatic electrophilic substitution.[28,29]

Similar conclusions can be drawn from the ^{1}H-NMR studies carried out with the SQ5 and SQ6 receptors by adding $AgNO_3$. As observed in the Fig. SI-5A and SI-5B,† the downfield chemical shift changes of the proton signals near the carbon attached to the sulfur atom, are lower than in the case of Hg^{2+}, but significant. The rest of the proton signals of the molecule, for both SQ5 and SQ6 receptors, are not affected at all.

In contrast, when performing similar experiments with the salts of $Pb(ClO_4)_2$, or $AuCl_3$, and the SQ5 and SQ6 receptors, respectively, no significant induced chemical shift changes of the proton signals in the ^{1}H-NMR were observed after 48 hours. These results lead us to suggest that the side chain containing a sulfur derivative scarcely participates in the recognition phenomenon of Pb^{2+} and Au^{3+} (see Fig. S6-A, S6-B, S7-A and S7-B†).

In order to find out the degree of participation of the carbonyl units of the squaramide unit in the complex formation between 3,4-dimetoxi-SQ1 and the Au^{3+} ions, a ^{13}C-NMR experiment was carried out, see Fig. SI-8.† Thus, upon the addition of $AuCl_3\cdot 3H_2O$ in CD_3CN, to a solution of 3,4-dimetoxi-SQ1 (1 : 1 ratio), a slight shift of the quaternary carbons signals corresponding to the C=O interacting with the Au^{3+} ion is observed. Even if very stable complexes are formed, the induced chemical shift change of these signals is difficult to observe, because quaternary carbons do not usually appear clearly in the spectra, unless the concentration of the complex is really high.

The coordination between SQ(5–7) and the different metal ions was confirmed using the Electrospray Ionization (ESI) technique in positive detection mode, in acetonitrile. In the experiment with the Hg^{2+} salt, the mono-charged positive ion of a 1 : 1 complex corresponding to $[Hg\cdot SQ5\text{-}H]^+$ stoichiometry was observed. For the Ag^+ cation, a 1 : 1 complex with stoichiometry $[Ag\cdot SQ5]^+$ and a 1 : 2 complex with stoichiometry $[Ag\cdot(SQ5)_2]^+$ could be detected. In the case of Pb^{2+}, we observed the mono-charged positive ion-peak that could be assigned to a 1 : 1 complex with stoichiometry $[Pb\cdot SQ5\text{-}H]^+$. In Fig. SI-9A and SI-9B,† the excellent correlation between the measured and calculated isotopic patterns for these complexes is shown. After different tests, the formation of the complexes between SQ(5 and 6) and the Au^{3+} ion could not be observed by ESI. Instead, unexpectedly appeared an ion-peak whose mass corresponded with the formation of the sulfoxide due to the oxidation of the thioether group of squarate SQ-6.

In light of this result, we decided to prepare two independent solutions of squaramides SQ5 and SQ6 in acetonitrile, and added an aqueous solution of $AuCl_3\cdot 3H_2O$. Right afterwards, we observed the precipitation of Au^0 nanoparticles in the medium due to the redox reaction that occurs between the Au^{3+} and the thioether group located on the receptors chains. This reaction also occurs in water, but not in DMSO, which is why it had not been previously observed. In Fig. 4 the progress of the reaction, followed by ^{1}H-NMR, with the progressive addition of different amounts of Au^{3+} metallic ion is shown. As expected, the corresponding singlet of the methyl linked to the sulfur atom (located at 2.1 ppm, signal 1) disappears as the amount of metallic ion increases, whereas a new signal appears at 3.0 ppm (1′), which corresponds to the methyl group located next to the new sulfoxide group. A similar situation occurs with the triplet signal corresponding to methylene group (signal 2), which practically disappears as the triplet of the CH_2 (signal 2′) located next to the sulfoxide group increases.

The formation of Au^0 nanoparticles is evident after the analysis of samples recovered by Energy Dispersive X-ray (EDX). In the microphotographs, shown in Fig. 5, it can be clearly observed the bright spots due to the presence of gold deposited upon FeNP-SQ2. In addition, the analysis of the composition of the sample clearly proves the presence of Au^0. The resolution of the SEM microphotographs is not clear-cut, because to make this analysis correctly it is required to cover the sample with gold, an operation totally incompatible with the phenomenon that we intend to observe.

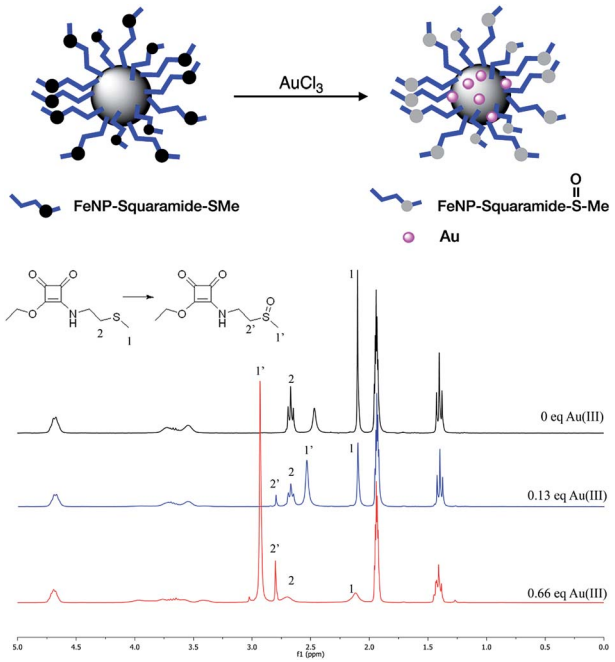

Fig. 4 Transformation of ethylthiomethyl into ethylmethylsulfoxide.

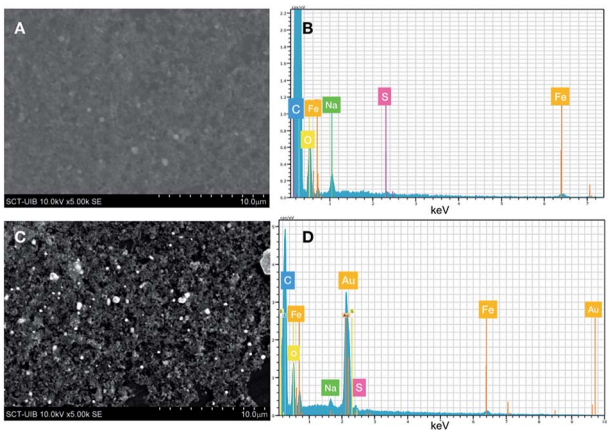

Fig. 5 SEM microphotographs and EDX analysis of FeNP-SQ2 and FeNP-SQ2@Au.

This result is very interesting since it allows obtaining a new gold-coated hybrid material of FeNP *in situ*, with a without the use of an external reducer, *e.g.*, sodium borohydride.[30]

The binding/absorption capacities of the hybrid nanomaterials were tested using experiments directed to the removal of Hg^{2+}, Pb^{2+}, Ag^{+}, Au^{3+} ions from aqueous solutions. To calculate the remaining concentrations in solution the ICP-OES technique was used. The Fig. 6 shows the percentages of retention obtained for the four new hybrid functionalized nanoparticles, FeNP-SQ(1–4), compared with the control iron nanoparticles, FeNP. Usually, retention percentages represent the amount of analyte removed from the solution by the hybrid nanoparticle, thus providing a good evaluation of the degree of relative binding/absorption between the hybrid material and the various target analyte. In Fig. 6, different retention

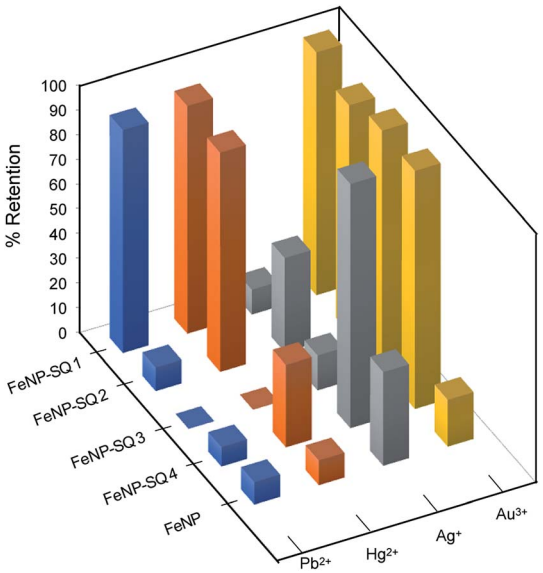

Fig. 6 Percentages of retention for different hybrid materials and metal ions, in water solution.

percentages can be observed, depending on the hybrid material and the metal ions tested. The FeNP-SQ1 hybrid material shows a 90% retention rate on Hg^{2+} and Pb^{2+} metal ions, even with a higher preference for the Au^{3+} metal ion, almost 100%. The decrease in the retention capacity of Pb^{2+} shown by the rest of the nanoparticles is quite surprising as well as the different retention percentages of Hg^{2+}. In addition, only one model of the tested ones, FeNP-SQ4, seems to be suitable for the interaction with Ag^{+}, with a quantitative retention of practically 100%, and very small retention rates for Hg^{2+} and Pb^{2+}. The good retention percentages observed between the hybrids receptors that have sulfur groups and the metal ion Au^{3+}, are assumed to be due to the reduction of Au^{3+} to Au^{0}.

To quantitatively compare the interaction between the different hybrid material models and the proposed metallic ions, the distribution constant K_d was calculated, expressed according to eqn (1).[31]

$$K_d = \frac{C_o - C_f}{C_f} \times \frac{V}{M} \quad (1)$$

The value of K_d (eqn (1)) represents the weighted partition coefficient of the analyte between the liquid (supernatant) and the solid phase (adsorbent), where the initial concentration of the analyte, C_f is the concentration of the analyte remaining in solution after extraction with the FeNP-SQ(1–4) or FeNP, V is the volume of solution used for the extraction experiment, in mL, and M is the mass of nanoparticles, FeNP, or hybrid iron nanoparticles used in the experiments, in g. The values obtained for the hybrid materials, shown in Table 3, are always larger than those corresponding to the FeNP unfunctionalized nanoparticles (control), thereby demonstrating the efficiency of the functionalization of the hybrid material: K_d values above 10^3 mL g^{-1} are considered to be very good and those that exceed 10^4 mL g^{-1} are considered as outstanding.[31]

Table 3 Calculated values for the distribution coefficients K_d (mL g^{-1}), measured in HNO_3 2%

	Au^{3+}	Ag^{+}	Pb^{2+}	Hg^{2+}
FeNP-SQ1	1.57×10^6	4.70×10^3	1.28×10^5	1.86×10^5
FeNP-SQ2	2.15×10^5	3.03×10^4	5.16×10^3	3.75×10^5
FeNP-SQ3	1.32×10^6	5.78×10^3	4.86×10^3	1.69×10^3
FeNP-SQ4	8.97×10^5	6.95×10^5	7.70×10^2	5.27×10^3
FeNP control	3.58×10^3	1.55×10^3	2.56×10^2	1.69×10^3

From the results shown in Table 3, it is once again established that the previously described model,[18] using the disquaramide SQ1, maintains high coordination values with Pb^{2+} and Hg^{2+} metal ions, regardless of the morphology and preparative method of the magnetic iron nanoparticles used. In this respect, and for the first time, a strong interaction of the hybrid material FeNP-SQ1 with Au^{3+} ion is observed. From the results obtained so far, we presume that this association occurs through coordination of the Au^{3+} metal ion to the carbonyl groups of the squaramide unit, as observed for the of Hg^{2+} and Pb^{2+} ions. The metal–ligand binding energy is mainly based on purely electrostatic cation–dipole interactions. The high distribution constant measured (1.57×10^6 mL g^{-1}) makes this hybrid material an effective alternative for the removal and recovery of this noble metal from an aqueous solution by magnetic filtration. To the best of our knowledge, this is the first time that the ability of squaramides to complex Au^{3+} ion metal is reported.

In contrast to this excellent result, the Ag^{+} metal ion shows poor coordination values with this FeNP-SQ1 hybrid nanomaterial, only 4.70×10^3 mL g^{-1}, a value comparable to that obtained with the control FeNP nanoparticles.

The distribution coefficients (Table 3) also show that the retention of the Au^{3+} ion with the hybrid materials, FeNP-SQ(2–4) is very high, between 10^5 to 10^6 mL g^{-1}. As we have already stated, this high retention is not due to the coordination between the hybrid materials with Au^{3+} ion, but to the reduction of Au^{3+} to Au^0 by oxidizing the sulfur derivative of the squaramide residue to sulfoxide.

The Au^0 nanoparticles thus generated are separated by filtration together with the FeNP-SQ(2–4)@Au before being measured in the ICP-OES.

Unexpectedly, except for the FeNP-SQ2, the hybrid materials functionalized with sulfur derivatives, *i.e.*, FeNP-SQ(3 and 4), show a relatively poor coordination with the Pb^{2+} and Hg^{2+} ions, with K_d values similar to those of the non-functionalized nanoparticles. A possible explanation for this fact could be due to the hydrophilicity of the SMe group present in the coating of the nanoparticle. In aqueous solution, hydrogen bonds are formed between thioether group and water molecules, causing a uniform "shell" that covers the organic residues and, thereby, the entire nanoparticle. Since Pb^{2+} ion does not interact with sulfur group, this metallic ion will not probably pass through the layer and reach the carbonyl squaramide binding sites, thus decreasing the supramolecular recognition phenomenon. The fact that the attaching of the organic receptors on the nanoparticle is not a uniform process, will allow part of the Pb^{2+} ion to coordinate the naked iron nanoparticle. In the case of Hg^{2+} ion, which does interact with the sulfur group, although weakly, it can "go through" the layer effectively when the coating of iron nanoparticle is formed by small molecules (FeNP-SQ2), but not when they are already larger, FeNP-SQ3 and FeNP-SQ4.

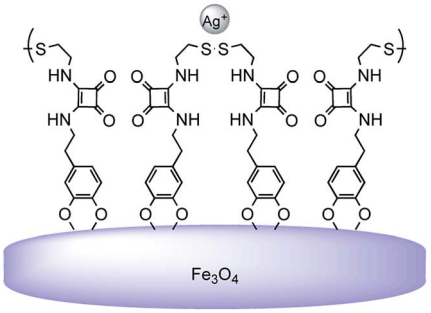

Fig. 7 Proposal of the interaction between FeNP-SQ4 and the Ag^{+} ions.

The hybrid nanoparticle FeNP-SQ1 is a special case: the butyl moiety attached to squaramide is a hydrophobic group and, in water solution, will allow the access of all the metallic ions to the hydrophilic carbonyl groups of the squaramide units.

Finally, the strong interaction found between FeNP-SQ4 and the Ag^{+} ion is significant. The ^{1}H-NMR experiments confirm that Ag^{+} ion interacts with the sulfur group of the receptors SQ5 and SQ6, and the experiments by ESI show the existence of the 1 : 1 complex $[(Ag{\cdot}SQ5)]^{+}$, which could explain the values of the distribution constant for FeNP-SQ2 and FeNP-SQ3. Moreover, the results obtained by ESI also demonstrate the existence of an ion-peak corresponding to a 1 : 2 complex $[Ag{\cdot}(SQ5)_2]^{+}$ (see Fig SI-10†). This result can be explained because the hybrid FeNP-SQ4 have two sulfur atoms (a disulfide group) which would favour the interaction of the organic residue with the metallic ion, thus increasing its retention capacity. This interacting scenario is shown in Fig. 7, where the organic disulfide squaramide is bent and anchored on the same nanoparticle, creating a macrocycle that would leave the two S atoms exposed to interact with Ag^{+} ions.

To test the stability of hybrid nanomaterials in water against the hydrolysis of catechol group, we carry out several Pdl measures, at different times after extraction experiments, without observing significant variations.

Conclusions

In summary, the process to obtain functionalized nanoparticles has been optimized with respect to previously published procedures, thanks to the application of the microwave technique, obtaining it easier, faster and cheaper, as well as considerably increasing its degree of functionalization on the nanoparticle, and therefore, its effectiveness.

Our results, retrieved by using different techniques, have demonstrated the ability of the carbonyl function of squaramide to operate as a receptor for metallic cations of different charge. It has been proved that the magnetic nanoparticles of

Fe_3O_4, functionalized with organosulfur-squaramide, are appropriate to effectively separate, by magneto filtration, ions from water, such as Hg^{2+}, Ag^{+}, and very especially the Au^{3+} cation. The process of removing Au^{3+} when the hybrid material contains a sulfur compound is associated with an oxidation–reduction reaction, carried out *in situ*, without the use of an external reducing agent, with formation and deposition of gold nanoparticles on the nanoparticle of Fe_3O_4. However, when the nanoparticle is functionalized with di-squaramides without sulfur atoms, the interaction with the Au^{3+} ion is carried out through the carbonyl groups of the squaramide unit.

Experimental

Materials and instruments

Reactions were carried out in oven-dried glassware under an atmosphere of argon, unless otherwise indicated. All commercially available reagents: diethyl squarate, dopamine hydrochloride, cystamine and 2-(methylthio)ethylamine were supplied by Sigma Aldrich. All the solvents were purchased from Scharlau and Fisher Chemicals. Acros Organics supplied $FeCl_2 \cdot 4H_2O$ and $FeCl_3$ anhydride. All the sodium salts carbonate and dithionite were purchased from Panreac. High purity water was generated by Milli-Q apparatus (Millipore).

^1H and ^{13}C NMR spectra were recorded on a Bruker Avance Spectrometer at 300 and 75 MHz at 23 °C. Chemical shifts are reported as parts per million (δ, ppm) referenced to the residual protium signal of deuterated solvents. Spectral features are tabulated in the following order: chemical shift (δ, ppm); multiplicity (s-singlet, d-doublet, t-triplet, m-multiplet and br-broad); number of protons. Electrospray mass spectra (HRMS-ESI) were recorded with a Micromass, Autospec3000 spectrometer provided with an electrospray module. Infrared (IR) were obtained on a Bruker Tensor 27 instrument in the solid state. Inductively Coupled Plasma Optical Emission Spectrometry (ICP-OES) assays were performed in a Perkin Elmer Optima 5300 DV instrument.

3-Ethoxy-4-((2-(methylthio)ethyl)amino)cyclobut-3-ene-1,2-dione

A solution of 2-(methylthio)etan-1-amine (200 mg, 2.19 mmol) in diethyl ether (20 mL) was added dropwise to a stirred solution of diethyl squarate (400 mg, 2.35 mmol) in diethyl ether (20 mL). The reaction mixture was stirred overnight at room temperature in an atmosphere of argon. After this period, a white precipitate appears. The solvent was decanted and the white product was cleaned with diethyl ether (3 × 20 mL), and finally dried under vacuum to obtain the desired product (324 mg, 70%). ^1H-NMR (DMSO-d_6) 8.86 (br, NH); 8.66 (br, NH); 4.66 (q, 2H); 3.66 (t, 1H); 3.47 (t, 3H); 2.64 (t, 2H); 2.07 (s, 3H); 1.37 (t, 3H) ppm. ^{13}C-NMR (DMSO-d_6) 188.93, 172.54, 172.24, 68.74, 33.98, 33.49, 15.49, 15.43, 14.26 ppm. IR (KBr): 3149, 2992, 1800, 1706, 1587, 1509, 1464, 1435, 1390, 1361, 1309, 1245, 1196, 1099, 1056, 1036, 1000, 821, 699, 614 cm^{-1}. HRMS-ESI(+) *m*/*z* calculated for $C_9H_{13}NO_3S$ $[M + Na]^+$ 238.0508, found 238.0500 and *m*/*z* calculated for $[2M + Na]^+$ 453.1130 found 453.1124.

3-((3,4-Dimethoxyphenethyl)amino)-4-ethoxycyclobut-3-ene-1,2-dione

A solution of 2-(3,4-dimethoxyphenyl)ethan-1-amine (1 g, 5.5 mmol) in diethyl ether (20 mL) was added dropwise to a stirred solution of diethyl squarate (1.12 g, 6.6 mmol) in diethyl ether (20 mL). The reaction mixture was stirred overnight at room temperature in an atmosphere of argon. After this period, a white precipitate appears. The solvent was decanted and the white product was cleaned with diethyl ether (3 × 10 mL), and finally dried under vacuum to obtain the desired product (1.41 g, 80%). ^1H-NMR (DMSO-d_6) 8.83 (br, NH); 8.62 (br, NH); 6.86 (d, 1H); 6.78 (s, 1H); 6.70 (d, 1H); 4.60 (q, 2H); 3.72 (s, 3H); 3.70 (s, 3H); 3.47 (t, 2H); 2.74 (bs, 2H); 1.33 (t, 3H) ppm. ^{13}C-NMR (DMSO-d_6) 189.22, 182.05, 176.7, 172.45, 148.64, 147.51, 130.66, 120.79, 112.74, 111.94, 68.76, 55.56, 55.37, 45.52, 44.89, 36.14, 35.83, 15.59 ppm. IR(KBr): 3206, 3078, 2986, 2937, 2831, 1799, 1698, 1597, 1501, 1453, 1385, 1354, 1267, 1234, 1192, 1156, 1142, 1103, 1049, 1030, 974, 935, 884, 829, 794, 768, 631, 562, 464 cm^{-1}. HRMS-ESI(+) *m*/*z* calculated for $C_{16}H_{19}NO_5$ $[M + Na]^+$ 328.1155, found 328.1150.

3-((3,4-Dimethoxyphenethyl)amino)-4-((2-(methylthio)ethyl)amino)cyclobut-3-ene-1,2-dione

A solution of 2-(methylthio)etan-1-amine (100 mg, 1.1 mmol) in ethanol (5 mL) was added dropwise to a stirred solution of 3-((3,4-dimethoxyphenethyl)amino)-4-ethoxycyclobut-3-ene-1,2-dione (341 mg, 1.12 mmol) in ethanol (25 mL). The reaction mixture was stirred overnight at room temperature in an atmosphere of argon. After this period, a white precipitate appears, the solution was cooled to increase the precipitation of product. The solvent was filtered and the white product was cleaned with cold ethanol (3 × 10 mL), and finally dried under vacuum to obtain the desired product (282 mg, 75%). ^1H-NMR (DMSO-d_6) 7.48 (br, NH); 6.87 (d, 1H); 6.83 (s, 1H); 6.73 (d, 1H); 3.73 (s, 3H); 3.71 (s, 3H); 2.77 (t, 2H); 2.63 (t, 2H); 2.07 (s, 3H) ppm, the signals of the $-CH_2-$ adjacent to the squaramidic group appear overlapping by the methoxy groups signals of the structure, within the interval from 4 to 3.5 ppm. ^{13}C-NMR (DMSO-d_6) 182.57, 182.44, 167.74, 148.63, 147.37, 130.86, 120.70, 112.68, 112.57, 111.9, 55.57, 55.45, 55.29, 44.63, 42.14, 36.48, 34.58, 14.42 ppm. IR (KBr): 3447, 3163, 2956, 1799, 1642, 1569, 1518, 1435, 1355, 1265, 1235, 1142, 1027, 806, 764, 601 cm^{-1}. HRMS-ESI(+) *m*/*z* calculated for $C_{17}H_{22}N_2O_4S$ $[M + Na]^+$ 373.1193, found 373.1193.

3-((3,4-Dihydroxyphenethyl)amino)-4-((2-(methylthio)ethyl)amino)cyclobut-3-ene-1,2-dione

A solution of 3-ethoxy-4-((2-(methylthio)ethyl)amino)cyclobut-3-ene-1,2-dione (61 mg, 0.28 mmol) in methanol (15 mL) was added dropwise to a stirred solution of dopamine hydrochloride (70 mg, 0.37 mmol), Na_2CO_3 (30 mg) and $Na_2S_2O_4$ (15 mg) in methanol (15 mL) basified to pH = 8 with NaOH (1 M). The reaction mixture was stirred overnight at room temperature in an atmosphere of argon and light protected with an aluminium foil. After this period, a white precipitate appears, the solution

was acidified with HCl (1 M). The solvent was removed under vacuum and the white product was cleaned with water (3 × 10 mL), cold methanol (3 × 10 mL) and diethyl ether (3 × 5 mL). Finally dried under vacuum to obtain the desired product (51 mg, 55%). ^{1}H-NMR (DMSO-d_6) 8.76 (s, OH); 8.67 (s, OH); 7.47 (br, NH); 6.63 (dd, 1H); 6.60 (ds, 1H); 6.6.45 (dd, 1H); 3.67 (t, 4H); 2.63 (t, 4H); 2.07 (s, 3H) ppm. ^{13}C-NMR (DMSO-d_6) 182.56, 182.44, 167.70, 167.65, 145.13, 143.72, 129.16, 119.38, 116.16, 116.08, 115.53, 44.87, 42.17, 36.44, 34.56, 14.44 ppm. IR (KBr): 3169, 2956, 1802, 1639, 1581, 1553, 1429, 1355, 1269, 1115, 951, 814, 606 cm^{-1} MS: HRMS-ESI(+) *m*/*z* calculated for $C_{15}H_{18}N_2O_4S$ $[M + Na]^+$ 345.0879, found 345.0879.

4,4′-((Disulfanediylbis(ethane-2,1-diyl))bis(azanediyl))bis(3-ethoxycyclobut-3-ene-1,2-dione)

In a first step, cystamine hydrochloride (1 g, 4.43 mmol) was dissolved in 40 mL of acetonitrile and mixed up with 2.5 mL (4 eq.) of triethylamine for two hours. In a second step, a solution of diethyl squarate (1.6 g, 9.4 mmol, 2.1 eq.) in 10 mL of acetonitrile was added to the initial solution. The reaction mixture was stirred overnight at room temperature in an atmosphere of argon. The solvent was removed in vacuum and the residue was dissolved in dichloromethane. The solution was cleaned with HCl 1M (2 × 10 mL). The organic solvent was removed under vacuum and the product was precipitated with dichloromethane and pentane. The solid was filtered and dried with diethyl ether (2 × 10 mL) to get the desired product (1.78 g, 51%). ^{1}H-NMR (DMSO-d_6) 8.87 (br, NH); 8.69 (br, NH); 4.65 (q, 2H); 3.76 (d, 1H); 3.58 (d, 3H); 2.89 (t, 2H); 1.36 (t, 3H) ppm. ^{13}C-NMR (DMSO-d_6) 189.11, 182.22, 176.97, 172.54, 68.92, 42.68, 37.94, 15.64 ppm. IR (KBr): 3445, 3166, 2954, 1799, 1645, 1574, 1517, 1436, 1351, 1263, 1235, 1155, 1141, 1026, 807, 764, 600 cm^{-1}. HRMS-ESI(+) *m*/*z* calculated for $C_{16}H_{20}N_2O_6S_2$ $[M + Na]^+$ 423.0655, found 423.0656.

4,4′-((Disulfanediylbis(ethane-2,1-diyl))bis(azanediyl))bis(3-((3,4 dimethoxyphenethyl)amino) cyclobut-3-ene-1,2-dione)

A solution of 2-(3,4-dimethoxyphenyl)ethan-1-amine (112 mg, 0.61 mmol) in methanol (20 mL) was added dropwise to a solution of 4,4′-((disulfanediylbis(ethane-2,1-diyl)) bis(azanediyl))bis(3-ethoxycyclobut-3-ene-1,2-dione) (100.86 mg, 0.25 mmol) in methanol (30 mL). The reaction mixture was heated to 50 °C for 30 minutes and left stirring for 2 hours. A white precipitate was decanted and washed with methanol under sonication. The desired product was obtained as a white precipitate (121 mg, 0.18 mmol, 75%). ^{1}H-NMR (DMSO-d_6) 7.53 (br, NH); 6.88 (d, 2H); 6.82 (s, 2H); 6.73 (d, 2H); 3.73 (s, 6H); 3.71 (s, 6H); 2.91 (t, 4H); 2.76 (t, 4H) ppm, the signals of the –CH_2– adjacent to the squaramidic group appear overlapping by the methoxy groups signals of the structure, within the interval from 4 to 3.5 ppm. ^{13}C-NMR (DMSO-d_6) 182.62, 182.38, 167.94, 167.43, 148.62, 147.36, 130.85, 120.67, 112.65, 111.89, 55.42, 44.70, 36.46 ppm. IR (KBr): 3164, 2952, 1799, 1646, 1574, 1517, 1434, 1351, 1293, 1263, 1235, 1154, 1141, 1026, 806, 764, 599 cm^{-1}. HRMS-ESI(+) *m*/*z* calculated for $C_{32}H_{38}N_4O_8S_2$ $[M + Na]^+$ 693.2023, found 693.2023.

4,4′-((Disulfanediylbis(ethane-2,1-diyl))bis(azanediyl))bis(3-((3,4dihydroxyphenethyl)amino)cyclobut-3-ene-1,2-dione)

A solution of 4,4′-((disulfanediylbis(ethane-2,1-diyl))bis (azanediyl))bis(3-((3,4 dimethoxyphenethyl) amino) cyclobut-3-ene-1,2-dione) (400 mg, 1 mmol) in methanol (25 mL) was added dropwise to a stirred solution of dopamine hydrochloride (400 mg, 2.11 mmol), Na_2CO_3 (200 mg) and $Na_2S_2O_4$ (400 mg) in methanol (25 mL) basified to pH = 8 with NaOH 1 M. The reaction mixture was stirred overnight at room temperature in an atmosphere of argon and light protected with an aluminium foil. The solvent was removed under vacuum and the white product was cleaned with water (3 × 10 mL) cold methanol (3 × 10 mL) and diethyl ether (3 × 5 mL). Finally dried under vacuum to obtain the desired product (453 mg, 68%). ^{1}H-NMR (DMSO-d_6) 6.62 (d, 2H); 6.60 (s, 2H); 6.45 (d, 2H); 3.77 (t, 4H); 3.65 (t, 4H); 2.92 (t, 4H); 2.64 (t, 4H) ppm. ^{13}C-NMR (DMSO-d_6) 182.63, 182.38, 167.88, 167.45, 145.13, 143.72, 129.15, 119.38, 116.16, 115.55, 44.93, 41.96, 36.44 ppm. IR (KBr): 3170, 2956, 1799, 1648, 1575, 1431, 1349, 1294, 1206, 1112, 1025, 951, 814, 755, 730, 610, 455 cm^{-1}. HRMS-ESI(+) *m*/*z* calculated for $C_{28}H_{30}N_4O_8S_2$ $[M + Na]^+$ 637.1397, found 637.1400.

3-Ethoxy-4-((2-(methylthio)propyl)amino)cyclobut-3-ene-1,2-dione

A solution of 2-(methylthio)propan-1-amine (175 mg, 1.66 mmol) in acetonitrile (10 mL) was added dropwise to a stirred solution of diethyl squarate (289 mg, 1.69 mmol) in acetonitrile (10 mL). The reaction mixture was stirred overnight at room temperature in an atmosphere of argon. After this period, the solvent was evaporated and the oil residue was dissolved in diethyl ether and left to cool overnight in the fridge. The desired product was obtained as a yellowish solid (302 mg, 79%). ^{1}H-NMR (DMSO-d_6) 8.79 (br, NH); 8.60 (br, NH); 4.65 (q, 2H); 3.55 (q, 1H); 3.37 (q, 1H); 2.45 (s, 2H); 2.04 (s, 3H); 1.77 (m, 2H); 1.37 (t, 3H) ppm. ^{13}C-NMR (DMSO-d_6) 189.25, 182.18, 176.80, 172.46, 68.76, 42.79, 30.04, 29.73, 29.21, 15.62, 14.51 ppm. IR (KBr): 3452, 3201, 2918, 2286, 2097, 1802, 1705, 1598, 1504, 1433, 1386, 1360, 1310, 1278, 1237, 1209, 1186, 1150, 1105, 1050, 1009, 991, 951, 872, 830, 816, 763, 698, 649, 618, 606, 407 cm^{-1}. HRMS-ESI(+) *m*/*z* calculated for $C_{10}H_{15}NO_3S$ $[M + Na]^+$ 252.0665 found 252.0657 and for $[2M + Na]^+$ 481.1437, found 481.1439.

3-((3,4-Dimethoxyphenethyl)amino)-4-((2-(methylthio)propyl) amino)cyclobut-3-ene-1,2-dione

A solution of 2-(methylthio)propan-1-amine (30 mg, 0.28 mmol) in ethanol (5 mL) was added dropwise to a stirred solution of 3-((3,4-dimethoxyphenethyl)amino)-4-ethoxycyclobut-3-ene-1,2-dione (70 mg, 0.23 mmol) in ethanol (20 mL). The reaction mixture was stirred overnight at room temperature in an atmosphere of argon. After this period, a white precipitate appears, the solution was cooled to increase the quantity of product. The solvent was filtered and the white product was cleaned with cold ethanol (3 × 10 mL) and finally dried under vacuum to obtain the desired product (61 mg, 73%). ^{1}H-NMR (DMSO-d_6) 7.48 (br, NH); 6.87 (d, 1H); 6.83 (s, 1H); 6.73 (d,

1H); 3.73 (s, 3H); 3.71 (s, 3H); 2.76 (t, 2H); 2.46 (d, 2H); 2.04 (s, 3H); 1.78 (m, 2H) ppm, the signals of the $-CH_2-$ adjacent to the squaramidic group appear overlapping by the methoxy groups signals of the structure, within the interval from 4 to 3.5 ppm. ^{13}C-NMR (DMSO-d_6) 182.45, 167.80, 148.63, 147.37, 130.88, 120.71, 112.67, 111.87, 55.51, 55.35, 44.67, 42.18, 36.50, 30.10, 29.98, 14.54 ppm. IR (KBr): 3453, 3165, 2949, 2839, 2197, 1799, 1645, 1574, 1518, 1431, 1358, 1292, 1264, 1235, 1154, 1141, 1026, 934, 856, 807, 764, 743, 634, 600, 461 cm^{-1}. HRMS-ESI(+) *m*/*z* calculated for $C_{18}H_{24}N_2O_4S$ $[M + Na]^+$ 387.1349, found 387.1349.

3-((3,4-Dihydroxyphenethyl)amino)-4-((2-(methylthio)propyl) amino)cyclobut-3-ene-1,2-dione

A solution of 3-ethoxy-4-((2-(methylthio)propyl)amino)cyclobut-3-ene-1,2-dione (300 mg, 1.3 mmol) in methanol (20 mL) was added dropwise to a stirred solution of dopamine hydrochloride (300 mg, 1.58 mmol), Na_2CO_3 (120 mg) and $Na_2S_2O_4$ (60 mg) in methanol (20 mL) basified to pH = 8 with NaOH 1 M. The reaction mixture was stirred overnight at room temperature in an atmosphere of argon and light protected with an aluminium foil. After this period, a white precipitate appears, the solution was acidified with HCl (1 M). The solvent was removed under vacuum and the white product was cleaned with water (3 × 10 mL) cold methanol (3 × 10 mL) and diethyl ether (3 × 5 mL) finally dried under vacuum to obtain the desired product (51 mg, 55%). ^{1}H-NMR (DMSO-d_6) 8.77 (s, OH); 8.69 (s, OH); 7.39 (br, NH); 6.64 (d, 1H); 6.60 (s, 1H); 6.45 (d, 1H); 3.64 (ds, 2H); 3.55 (ds, 2H); 2.66 (t, 2H); 2.04 (s, 3H); 1.77 (t, 2H) ppm. ^{13}C-NMR (DMSO-d_6) 182.44, 167.76, 145.62, 144.18, 128.86, 119.05, 116.03, 115.38, 44.93, 42.18, 36.50, 30.09, 29.99, 14.54 ppm. IR (KBr): 3170, 2955, 1799, 1649, 1582, 1486, 1433, 1354, 1279, 1199, 1150, 1113, 1069, 1025, 952, 869, 815, 755, 633, 613 cm^{-1}. HRMS-ESI(+) *m*/*z* calculated for $C_{16}H_{20}N_2O_4S$ $[M + H]^+$ 337.1217, found 337.1215.

Synthesis of magnetic nanoparticles by co-precipitation method

A solution of NaOH 1M (7 mL) was added slowly to a stirred solution of $FeCl_3$ (160 mg) and $FeCl_2 \cdot 4H_2O$ (100 mg) in water (5 mL). The addition was carried out in atmosphere of argon for 15–20 minutes. When the addition has finished, the mixture was left to keep stirring for 20 minutes. When the time has finished, the black precipitate was decanted by magnetic attraction and washed with water until a neutral pH. Finally, nanoparticles were cleaned with methanol to remove water, and suspended in 10 mL of methanol. IR (KBr): 3418, 1626, 1457, 1343, 1115, 1071, 934, 854, 808, 616, 453 cm^{-1}.

Functionalization of magnetic nanoparticles

In a 2–5 mL microwave vessel, 3 × 10^{-2} mmol of the desired dopamine derivate receptor were added. The di-squaramide was dissolved in DMSO (1 mL). Following, a homogeneous suspension of magnetic nanoparticles, FeNP, (10 mg mL^{-1}) in methanol was added (1 mL), the mixture was diluted to 5 mL with methanol. The vessel of reaction was hermetically closed and inserted in the microwave. The reaction was carried out for 20 minutes at 120 °C, with a pressure about 3 bar. After reaction, functionalized magnetic nanoparticles were cleaned with water (3 × 10 mL) and suspended in 10 mL of water.

FeNP with 3-((3,4-dihydroxyphenethyl)amino)-4-((2-(methylthio) ethyl)amino)cyclobut-3-ene-1,2-dione

IR (KBr): 3419, 2922, 2952, 1800, 1633, 1590, 1542, 1483, 1427, 1384, 1352, 1262, 1210, 1117, 1020, 809, 578, 438 cm^{-1}.

FeNP with 4,4′-((disulfanediylbis(ethane-2,1-diyl))bis(azanediyl)) bis(3-((3,4-dihydroxyphenethyl)amino)cyclobut-3-ene-1,2-dione)

IR (KBr): 3418, 2924, 1799, 1652, 1590, 1540, 1482, 1434, 1349, 1264, 1119, 1022, 812, 602, 453 cm^{-1}.

FeNP with 3-((3,4-dihydroxyphenethyl)amino)-4-((2-(methylthio) propyl)amino)cyclobut-3-ene-1,2-dione

IR (KBr): 4322, 2923, 2853, 1799, 1646, 1592, 1546, 1486, 1434, 1384, 1352, 1267, 1219, 1024, 879, 814, 579 cm^{-1}.

Conflicts of interest

There are no conflicts to declare.

Acknowledgements

This work was supported by MINECO/AEI of Spain (projects CTQ2014-57393-C2-1-P and CTQ2017-85821-R, FEDER funds). Paulino Duel acknowledges his PhD scholarship from Conselleria d'Innovació, Recerca I Turisme del Govern de les Illes Balears. M. Susana Gutiérrez acknowledges her PhD scholarship from CONACyT (Consejo Nacional de Ciencia y Tecnología de México). Paulina Rodríguez acknowledges her scholarship from Fundación Carolina. Alberto León acknowledges his financial support from Programa SOIB Jove-Qualificats Sector Públic (Govern de les Illes Balears).

References

1 https://ec.europa.eu/environment/circular-economy/index_en.htm, Consulted on March 18, 2018.
2 *The maximum concentration allowed for the silver in the drinking water by the US EPA are: 50 μg/L. Ambient Water Quality Criteria for Silver*, Environmental Protection Agency, Office of Water, Washington, DC, 1980, EPA 440/5-80-071.
3 *The maximum concentration allowed for the mercury in the drinking water by the US EPA are: 0.002 μg/L. Ambient Water Quality Criteria for Mercury*, U.S. Environmental Protection Agency, Office of Water, Washington, DC, 1985, EPA 440/5-94-026.
4 *The maximum concentration allowed for the lead in the drinking water by the US EPA are: 0.0015 μg/L. Ambient Water Quality Criteria for Lead*, U.S. Environmental Protection Agency, Office of Water, Washington, DC, 1985, EPA 440/5-84-027.
5 There is no clear criterion established regarding the maximum allowed concentration of gold in the drinking water.

6 A. Rubo, R. Kellens, J. Reddy, N. Steier and W. Hasenpusch, *Ullmann's Encyclopedia of Industrial Chemistry*, Wiley-VCH Verlag GmbH, 2000.
7 Z. Liu, M. Frasconi, J. Lei, Z. J. Brown, Z. Zhu, D. Cao, J. Iehl, G. Liu, A. C. Fahrenbach, Y. Y. Botros, O. K. Farha, J. T. Hupp, C. A. Mirki and J. F. Stoddart, *Nat. Commun.*, 2013, **4**, 1855.
8 Z. Liu, A. Samamta, J. Lei, J. Sumg, Y. Wang and J. F. Stoddart, *J. Am. Chem. Soc.*, 2016, **138**, 11643–11653.
9 M. Mon, J. Ferrando-Soria, T. Grancha, F. R. Fortea-Pérez, J. Gascon, A. Leyva-Pérez, D. Armentano and E. Pardo, *J. Am. Chem. Soc.*, 2016, **138**, 7864–7867.
10 R. De Palma, S. Peeters, M. J. Van Bael, H. Van den Rul, K. Bonroy, W. Laureyn, J. Mullens, G. Borghs and G. Maes, *Chem. Mater.*, 2007, **19**, 1821–1831.
11 A. M. Demin, V. P. Krasnov and V. N. Charushin, *Mendeleev Commun.*, 2013, **23**, 14–16.
12 D. Ling, W. Park, Y. I. Park, N. Lee, F. Li, C. Song, S.-G. Yang, S. H. Choi, K. Na and T. Hyeon, *Angew. Chem., Int. Ed.*, 2011, **123**, 11562–11567.
13 A. K. L. Yuen, G. A. Hutton, A. F. Masters and T. Maschmeyer, *Dalton Trans.*, 2012, **41**, 2545–2559.
14 K. A. López, M. N. Piña, R. Alemany, O. Vögler, F. Barceló and J. Morey, *RSC Adv.*, 2014, **4**, 19196–19204.
15 S. Sun and H. Zeng, *J. Am. Chem. Soc.*, 2002, **124**, 8204–8205.
16 W. Yantasee, C. L. Warner, T. Sangvanich, R. S. Addleman, T. G. Carter, R. J. Wiacek, G. E. Fryxell, C. Timchalk and M. G. Warner, *Environ. Sci. Technol.*, 2007, **41**, 5114–5511.
17 C. L. Warner, R. S. Addleman, A. D. Cinson, T. C. Droubay, M. H. Engelhard, M. A. Nash, W. Yantasee and M. G. Warner, *ChemSusChem*, 2010, **3**, 749–757.
18 K. A. López, M. N. Piña, D. Quiñonero, P. Ballester and J. Morey, *J. Mater. Chem. A*, 2014, **2**, 8796–8803.
19 M. S. Gutiérrez, P. Duel, F. Hierro, J. Morey and M. N. Piña, *Small*, 2018, **14**, 1702573.
20 H. Häkkinen, *Nat. Chem.*, 2012, **4**, 443–455.
21 Y. Xue, X. Li, H. Li and W. Zhang, *Nat. Commun.*, 2014, **5**, 4348.
22 D. Quiñonero, K. A. López, P. M. Deyà, M. N. Piña and J. Morey, *Eur. J. Org. Chem.*, 2011, 6187–6194.
23 K. A. López, M. N. Piña and J. Morey, *Synlett*, 2012, **23**, 2830–2834.
24 F. Benyettou, E. Guenin, Y. Lalatonne and L. Motte, *Nanotechnology*, 2011, **22**, 055102.
25 O. Pascu, E. Carenza, M. Gich, S. Estradé, F. Peiró, G. Herranz and A. Roig, *J. Phys. Chem. C*, 2012, **116**, 15108–15116.
26 M. Gutiérrez, M. N. Piña, K. López and J. Morey, *RSC Adv.*, 2017, **7**, 19385–19390.
27 L. Martínez, G. Martorell, A. Sampedro, P. Ballester, A. Costa and C. Rotger, *Org. Lett.*, 2015, **17**, 2980–2983.
28 H. Satub, K. P. Zeller and H. Leditsche, *Houben-Weyl's, Methoden der Organischen Chemie*, Georg Thieme Verlag, Stuttgart, 4th edn, 1974, vol. 13, pt 2b, pp. 28–59.
29 L. G. Makarova and A. N. Nesmeyanov, *The organic compounds of mercury*, North-Holland Publising Co., Amsterdam, 1967, pp. 71–121.
30 P. Miao, Y. Tang and L. Wang, *ACS Appl. Mater. Interfaces*, 2017, **9**, 3940–3947.
31 G. E. Fryxell, Y. Lin, S. Fiskum, J. C. Birnbaum, H. Wu, K. Kemner and S. Kelly, *Environ. Sci. Technol.*, 2005, **39**, 1324–1331.